UC San Diego
UC San Diego Electronic Theses and Dissertations

Title

Contribution of the Retrosplenial Cortex to Spatial Working Memory

Permalink

https://escholarship.org/uc/item/0rj632dv

Author

Parikh, Sagar Jwalant

Publication Date

2022

Peer reviewed|Thesis/dissertation

UNIVERSITY OF CALIFORNIA SAN DIEGO

Contribution of the Retrosplenial Cortex to Spatial Working Memory

A Thesis submitted in partial satisfaction of the requirements
for the degree Master of Science

in

Biology

by

Sagar Jwalant Parikh

Committee in charge:

Professor Douglas Nitz, Chair
Professor Cory Root, Co-Chair
Professor Brenda Bloodgood

2022

The Thesis of Sagar Jwalant Parikh is approved, and it is acceptable in quality and form for publication on microfilm and electronically.

University of California San Diego

2022

DEDICATION

This thesis is dedicated to the incredible rats who contribute their lives to helping us

better understand the brain and how it functions.

TABLE OF CONTENTS

LIST OF FIGURES

LIST OF TABLES

LIST OF ABBREVIATIONS

RSC   Retrosplenial Cortex

M2   Secondary Motor Cortex

RDG   Dysgranular Retrosplenial Cortex

RSG   Granular Retrosplenial Cortex

HD   Head Direction

TTT   Triple-T

DREADD   Designer Receptor Exclusively Activated by Designer Drug

CNO   Clozapine-N-Oxide

AAV   Adeno-Associated Virus

AP   Anterior/Posterior

ML   Medial/Lateral

Z   Dorsal/Ventral

CTR   Control

SAL   Saline

ACKNOWLEDGEMENTS

ABSTRACT OF THE THESIS

Contributions of the Retrosplenial Cortex to Spatial Working Memory

by

Sagar Jwalant Parikh

Master of Science in Biology

University of California San Diego, 2022

Professor Douglas Nitz, Chair
Professor Cory Root, Co-Chair

The retrosplenial cortex (RSC) is a unique brain structure that forms what is widely considered a hub of neuronal connections and interactions in the brain. Previous studies have implicated the RSC in contextual processing and discrimination, spatial memory, and learning (Keene & Bucci, 2008a; Keene & Bucci, 2008b; Smith et al., 2012; van Groen et al., 2004). Sill, the functions of the retrosplenial cortex in spatial working memory are not very well understood. Here, we investigate the contributions of the RSC to performance on a

challenging spatial working memory task via chemogenetic inhibition of RSC neurons. Using this approach, we transiently silenced neurons of the RSC while animals underwent testing on the Triple-T (TTT) maze in multiple task variations. The nature of the TTT maze allows for the expansion of an already complex task, presenting the animals with a uniquely challenging spatial working memory task. Ultimately, we found that inactivation of RSC neurons resulted in a moderate impairment in task performance on the TTT maze, with the most robust effect occurring on the most challenging and recently learned version of the task. Ultimately, these findings suggest that the RSC contributes to performance on a challenging spatial working memory task and may be particularly important for performance on recently learned navigational tasks.

INTRODUCTION

Anatomy

In rats, the retrosplenial cortex (RSC) comprises the entire posterior cingulate cortex and lies along the midline of the cerebrum, arching around the dorsocaudal half of the corpus callosum (Vogt & Peters, 1981; Witter et al., 2011). The RSC is commonly divided into the granular and dysgranular regions, with anatomical differences between the granular and dysgranular RSC such as different cell organization and sizes of cortical layers (Vogt & Peters, 1981; Vogt et al., 2004; Wyss and van Groen, 1992). Afferent connections to and efferent projections from the RSC have also been found to differ between the granular and dysgranular layers of the RSC (Witter et al., 2011).

There are three anatomical features that make the retrosplenial cortex particularly interesting when studying spatial cognition. First, the RSC is a hub of neuronal connections, making it capable of integrating many different types of information from different parts of the brain (Witter et al., 2011; Wyss and van Groen, 1992). Secondly, it sits at the juncture of the hippocampal formation and the cortex, a position that may allow the structure to translate spatial cognition into action (Wyss and van Groen, 1992). The translation of spatial cognition into action occurs during navigational tasks, making the RSC of particular interest when studying navigation. Finally, the RSC has specific and extensive connections to the secondary motor cortex (M2), which encodes current left/right turning behavior and upcoming left/right turning behavior, suggesting that the RSC may contribute to decision making and planning (Shibata et al., 2004; Sul et al., 2011).

RSC Connectivity

The RSC has been shown to have extensive connections with spatial and visual systems, the anterior thalamic nuclei, parietal cortex, and a variety of regions in the hippocampal formation and parahippocampal region (Wyss and van Groen, 1992; Witter et al., 2011). Previous studies have also found strong intrinsic connections within the subdivisions of the retrosplenial cortex (Witter et al., 2011). The dysgranular RSC (RDG) has reciprocal connections with the orbital cortex, multiple thalamic nuclei, and subcortical regions, while the granular RSC (RSG) has been found to receive inputs from the dorsal subiculum, claustrum, anterior cingulate cortex, and the anterior thalamus (Wyss and van Groen, 1992; Brennan et al., 2021).

Importantly, the RSC has dense interconnections with various structures in the hippocampal formation and parahippocampal region. The dysgranular RSC has been found to have projections to the perirhinal cortex, with reciprocal connections to the subiculum, postsubiculum, and entorhinal cortex (Wyss and van Groen, 1992; Vann et al., 2009). Meanwhile, RSG receives input from area CA1 and the subiculum, has reciprocal connections with the postsubiculum, and projects to the presubiculum, parasubiculum, and entorhinal cortex (Yamawaki et al., 2019; Wyss and van Groen, 1992). The retrosplenial cortex has also been found to have reciprocal connections with the anterior and laterodorsal thalamic nuclei (Vann et al., 2009; Yamawaki et al., 2019).

These thalamic nuclei, hippocampal, and parahippocampal structures have been implicated in a variety of tasks that require spatial cognition and have firing patterns that signal involvement in spatial working memory and decision-making tasks. Place cells (encode the animal's specific location in its environment) have been discovered in the hippocampus proper, entorhinal cortex, parasubiculum, and subiculum, while head direction cells have been found in

the postsubiculum, laterodorsal thalamic nucleus, and anterior thalamic nucleus (O'Keefe & Dostrovsky, 1971; Quirk et al., 1992; Taube, 1995a; Sharp & Green, 1994; Taube, 1995b; Blair & Sharp, 1995; Mizumori & Williams, 1993). Dense interconnections with structures that have been implicated in spatial working memory and navigation suggests that the RSC may also contribute to spatial and navigational behavior.

The RSC has also been found to have prominent outputs to the secondary motor cortex (M2; Vogt & Miller, 1983; Yamawaki et al., 2016). Previous studies have implicated M2 in predicting navigational decisions and discriminating specific navigational motor acts independently of spatial context, implicating this region in the planning of motor movements (Sul et al., 2011; Olson et al., 2020). Extensive connections to this region suggest that the RSC may also play a role in the translation of spatial cognition into action.

Ultimately, the connections of the RSC with structures encoding spatial and contextual information and the secondary motor cortex suggest that the RSC may receive and process spatial information and provide this information to M2. Thus, the anatomy of the RSC is perfectly designed to support decision-making in navigational tasks through areas such as M2.

Head Direction and Navigation

As mentioned, the RSC has dense connections with multiple brain regions known to have head direction (HD) cells. Lesions of the RSC have implicated the region in processing head direction signals from the anterodorsal thalamus and integrating visual information into the head direction circuit (Clark et al., 2010). The retrosplenial cortex has also been found to have HD cells itself (~10% of RSC neurons), in addition to cells that respond to other spatial-navigational variables such as place, angular velocity, and running speed (Chen et al., 1994; Cho & Sharp, 2001). Some neurons of RSG were found to receive directional and spatial input from the

anterior thalamus and dorsal subiculum, a pathway that is suggested to form a switch of rotational speed and directional information across brain hemispheres (Brennan et al., 2021). RSC lesions have also been found to have subtle effects on learning heading vectors, an understandable result due to the dense connections with thalamic nuclei that also relay head direction information to the hippocampal formation (Vann & Aggleton 2004). Additionally, the RSC has been found to fire with spatial periodicity, playing a role in compartmentalizing complex routes and encodes the distance from each position in a route to other positions (Alexander & Nitz, 2017). The RSC has also been found to encode an animal's position in egocentric and route-centered space, as well as the track location in allocentric space (Alexander & Nitz, 2015). Collectively, these results further implicate the RSC in spatial cognition and navigation.

Spatial Working Memory Tasks

The presence of HD cells in the RSC and dense connections between the region and other structures containing HD and place cells implicate the RSC as a contributor to spatial cognition. Many studies have utilized spatial working memory tasks coupled with lesions or recordings of activity in the RSC to better understand its contributions to spatial working memory specifically.

One of the paradigms most commonly used to assess the role of brain structures in spatial working memory is the T-maze alternation task. The T-maze has been used in cognitive research for over a century to study a variety of processes and phenomena. Its normally associated task requires animals to remember their most recent decision and alternate each trial to maximize the acquisition of rewards. This makes the T-maze and its task suitable for research on spatial working memory. As a result, the T-maze has been used in numerous lesion and recording studies to identify the functional roles of neuron populations in many brain structures.

For example, hippocampal damage was found to significantly impair the ability to alternate on the T-maze, suggesting this region is necessary to perform working memory tasks (Olton, 1986). More recent research has used the T-maze in conjunction with neuron recordings, revealing that hippocampal CA1 cells construct representations for behaviors and locations based on what has happened prior to a trial and what will happen afterwards (Wood et al., 2000).

Some studies with the T-maze have also implicated the RSC in spatial working memory and navigation. In a virtual T-maze alternation paradigm with head-fixed mice, Franco & Goard (2021) uncovered an anterior-posterior organization of connectivity in the RSC that represents environmental context and motor planning. That is, the researchers found that the posterior RSC encodes context and motor bias due to previously run trials, while the medial and anterior RSC regions encode motor planning signals prior to a decision point (Franco & Gourd, 2021). Ultimately, these results implicate the RSC in the performance of spatial working memory tasks and give specificity to its functions within those tasks.

Transient lesions of the RSC have been shown to disrupt the use of directional and allocentric information during the performance of a T-maze alternation task (Nelson et al., 2015a). Specifically, deficits in behavior occurred when the maze was rotated so that intra-maze and extra-maze cues conflicted, indicating that lesions of the RSC either force the animal to significantly rely on intra-maze cues or decrease its ability to shift away from the utilization of these cues (Nelson et al., 2015a). Lesions of the RSC have also been found to impair incidental spatial learning, sensory preconditioning, contextual learning, memory, and contextual processing (Nelson et al., 2015b; Fournier et al., 2020; Keene & Bucci 2008a; Keene & Bucci 2008b; Pothuizen & Aggleton, 2008).

The eight-arm radial maze is another maze commonly used to study spatial working memory. Usually, its task requires animals to collect rewards at each of the eight arms prior to readministration of the rewards (Olton & Samuelson, 1976). That is, for rewards to be replaced, the animal must visit each reward location at least once. Manipulations of this maze and its task allow for deeper investigation of the functional anatomy involved in spatial working memory tasks. For example, the maze, the reward locations, and the animal can all be rotated relative to the greater room environment. A prior study involved manipulating the orientation of maze elements or the animal relative to the room environment and included a delay between trials in one of its iterations, in addition to a lesion of the retrosplenial cortex for the experimental group (Vann & Aggleton, 2004). Ultimately, the study found that animals with retrosplenial lesions had a deficit in task performance, with the most robust effect occurring when the maze was rotated relative to the environment of the room putting intramaze and distal allocentric cues in conflict (Vann & Aggleton, 2004). Ultimately, this suggests that animals less readily utilize contextual information upon inhibition of the retrosplenial cortex.

T Maze Adaptations and the TTT Maze

Despite its application in working memory research, the T-maze involves a very simple task, demanding lesser cognitive engagement than other tasks. As a result, the T-maze has been manipulated to create more versatile and complex working memory tasks, further revealing the functions of brain structures during these tasks. For example, Frank et al. (2000) created a W track with a task requiring the animal to remember which outer arm of the maze it had most recently visited to correctly make the next decision–an extension of the T-maze working memory task but enabling continuous motion of the animal. Grieves et al. (2016) take this a step further, creating a Y maze with four potential routes to a total of three distinct reward locations. This

study investigated the firing rates of hippocampal place cells during the Y maze task and discovered a modulation of place fields while animals ran different routes to the same reward location, implicating these cells in encoding routes instead of goals (Grieves et al., 2016).

Another more complex adaptation of the T-maze is the double-Y maze used by Ainge et al. (2007). This maze consisted of four routes to four goal locations, where two of the locations were rewarded for several trials, then the reward locations were changed (Ainge et al., 2007). Like the W and Y mazes previously discussed, this maze and its paradigm helped uncover trajectory encoding of place cells in the hippocampus. The increased complexity of these mazes in relation to the T-maze allows for deeper investigation into the anatomy behind spatial working memory. Still, although they have more demanding working memory tasks, these T-maze adaptations have structured, trained behaviors that may not utilize their paradigm's full potential.

Notably, the double-Y maze previously mentioned slightly resembles the initial condition of the TTT maze (Figure 1A & 1B). However, in the TTT maze the behavioral demands of the animal are much more complex, allowing for the investigation of more complex spatial cognition via lesions or neuronal recordings. The TTT maze and its associated tasks are uniquely advantageous because they allow for the animals to engage in alternation behavior (like in the T-maze), but the animal cannot rely on this alternation alone to solve the tasks (See Methods). Additionally, the animals must create their own strategies to remember not only the previous decision, but up to seven decisions to solve the task because they must collect all (four or eight) of the rewards before rewards are readministered (See Methods).

<u>DREADD Inhibition</u>

In this experiment we used a chemogenetic manipulation (DREADD) to inhibit neurons in the retrosplenial cortex. "DREADDs" stands for designer receptor exclusively activated by designer drugs (Armbruster et al., 2007). DREADD manipulations provide a few advantages when compared to other more extensive lesions. First, chemogenetic manipulations are much less invasive than other procedures, as they do not require large cranial implants or physical damage to the brain (Smith et al., 2016). Additionally, chemogenetic manipulations allow us to use each animal as its own control, transiently inhibiting neurons with binding of the ligand to the receptor, after which the animals recover over time. The inhibitory receptor used in this experiment is exclusively bound by the drug clozapine-N-oxide (CNO), which is administered 45 minutes before a recording begins via intraperitoneal injection (See Methods).

In our experiment, we use the DREADDs virus AAV8.hSyn.hM4Di.mCherry (Duke University). AAV8 is an adeno associated virus (serotype 8), which enables efficient delivery of the accompanying components to desired neuron populations. The virus targets the human synapsin 1 promoter (hSyn), which enables long-term neuron specific viral expression (Kügler et al., 2003). "hM4Di" is a synthetic adaptation of the endogenous M4 muscarinic acetylcholine receptor, which will be expressed by neurons transfected by the virus (Armbruster et al., 2007). When this receptor is bound by a specific ligand (CNO), neurons expressing the virus are effectively silenced as the membrane becomes hyperpolarized via a decrease in cAMP signaling and an increase in activation of inward-rectifying potassium channels (Armbruster et al., 2007). Finally, mCherry is a fluorescent reporter that enables us to assess expression of the virus through histological procedures and evaluation under a fluorescent microscope.

While the role of the RSC in spatial working memory has been previously investigated, previous studies rely on simple alternation tasks or more complex mazes with simple behaviors. Due to the complex and unique nature of the TTT maze and its behavioral task, this experiment offers more insight into the role the RSC may play in navigation and spatial working memory. In particular, the complexity of the behavior allows us to draw more information out of the task by examining a variety of navigational variables that cannot be investigated with simpler paradigms. Additionally, our chemogenetic manipulation of the RSC using a DREADDs virus enables transient inhibition of the region, allowing us to use animals as their own controls and examine how an individual animal's decision-making strategy changes after the administration of CNO and inhibition of neurons in the RSC. Here, we hope to draw more specific conclusions about the nature of the RSC's role in challenging spatial working memory tasks and can do so due to the complexity of the TTT paradigm and the benefits of chemogenetic manipulations. With consideration of previous studies that have implicated RSC in working memory tasks and the integration of contextual information, I hypothesize that a chemogenetic inhibition of RSC neurons will cause a deficit in performance on the TTT maze.

METHODS

Subjects

All experimental protocols adhered to AALAC guidelines and were approved by IACUC and the UCSD Animal Care Program. Subjects were adult male Sprague-Dawley rats (n=7). Rats were housed individually and kept on a 12-h light/dark cycle throughout the experiment. Prior to training, the animals were habituated to the colony room and handled for acclimation for 1–2 weeks. After this, animals were placed on food restriction for motivational purposes until they reached 85–90% free-fed weight. Water was available without restriction.

Behavioral Apparatus and Experimental Room

All behavioral tasks were conducted on the "Triple-T" track maze (Figure 1). The Triple-T (TTT) maze is an environment made of black plastic with a running surface of a thin sheet of black rubber. This path network is made of tracks that are 8cm in width. The dimensions of the environment are 1.6m x 1.25m, elevated 20cm from the ground. Track edges are approximately 2cm in height, allowing for an unobstructed view of the distal cues and surrounding environment. Taller 10cm walls were included along the internal paths to block potential shortcuts across small gaps between tracks near the reward locations. Internal route lengths were 140 cm in total length, with turns at 51 cm, 87 cm, and 118 cm. Return route (from reward location to starting point) lengths varied based on the internal route that preceded them. Rewards (~1/3 piece of Honey Nut Cheerios cereal) were manually delivered at the reward sites. A single recording room with consistently dimmed lights was used throughout the behavioral training and experimental stages. The TTT maze was placed in the same location relative to the room environment during training and recordings. Fixed spatial cues on the walls ensured consistent spatial relationships across recording days.
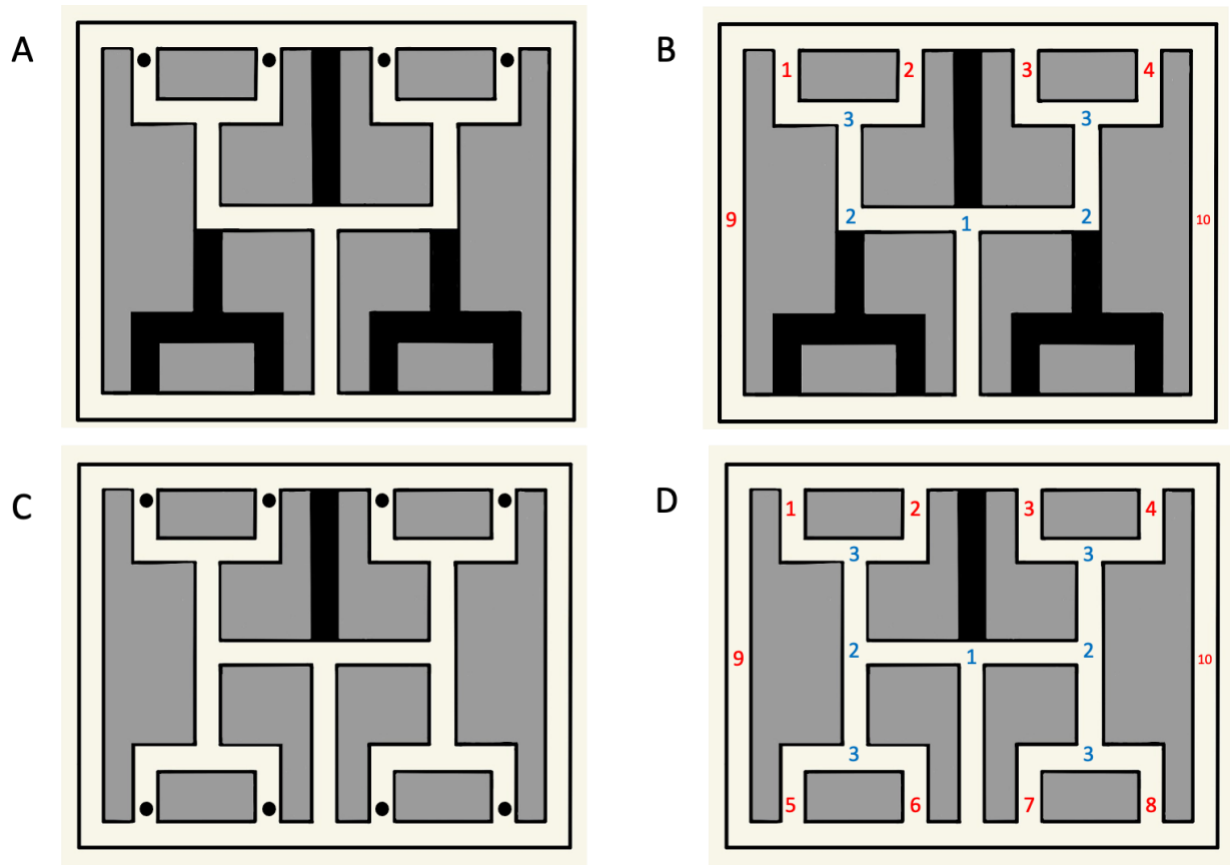
Figure 1: Illustration of the TTT Maze for its two tasks. Areas in black are blocked and unavailable to the animal. Black circles on the maze represent reward locations. Numbers listed in red indicate route numbers. Numbers listed in blue indicate turn numbers. (A,B) TTT Maze under the visit-only-4 task. (C,D) TTT Maze under the visit-all-8 task.

<u>Behavioral Training</u>

Rats were acclimated to the Triple-T maze through two 30-minute free exploration sessions. This was followed by the gradual introduction of each of the maze's elements over the course of 1-2 weeks. First, the cans used to stop the animal at the reward locations were introduced. Once the animals were acclimated to the cans, the 10cm walls were introduced to block sensory reward cues and shortcuts across paths. With all elements of the paradigm present, the animals were trained to run from the start location to one of the eight reward locations near the perimeter of the maze. The eight internal routes consisted of multiple straight sections with

11

three turns leading to a full stop at a goal location. The animal must then travel along the perimeter of the maze to the start location to begin a new trial.

Once the animal displayed efficient traversals of one path, the maze was opened to the four internal routes with reward locations furthest from the starting point. At this point in training, we implemented the visit-only-4 working memory task to be used throughout experimentation (Figure 1A & 1B). The animals were rewarded at any of the four locations but needed to visit all four locations before rewards were readministered at the four reward locations. Animals were not trained on the visit-all-8 paradigm and were exclusively exposed to the visit-only-4 paradigm during the training stage (Figures 1 & 2). Over at least two additional weeks, animals were trained by simple trial and error to a criterion of approximately one error per block. Animals underwent surgical delivery of the virus only after this level of task performance was achieved (Figure 2).
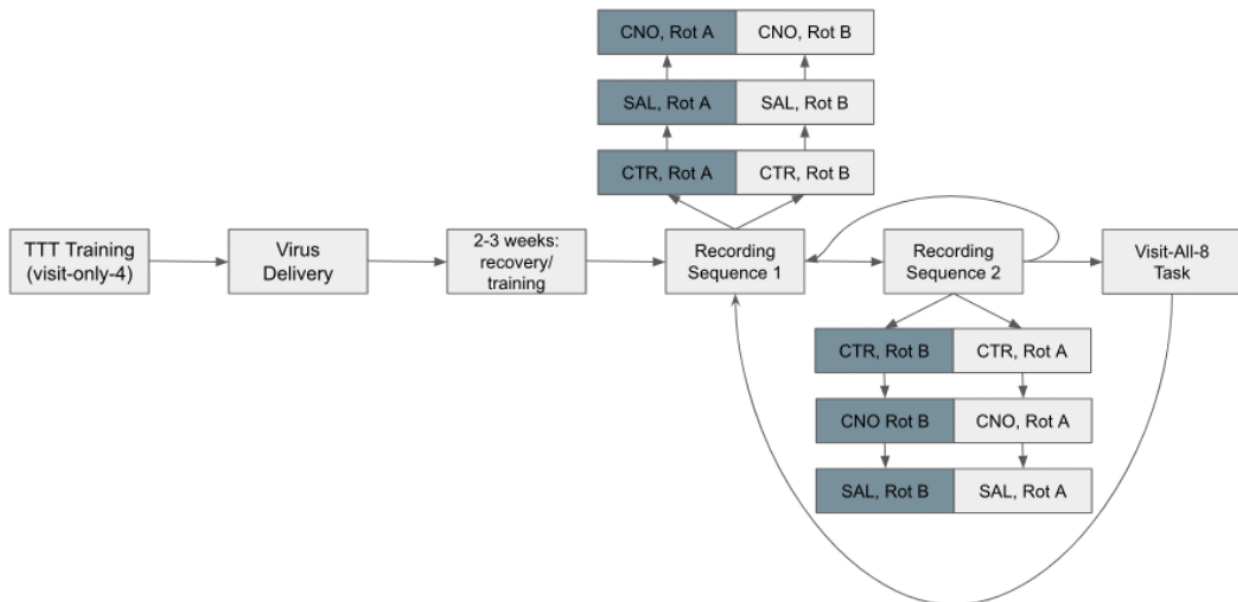
Figure 2: Schematic of experimental design. Training on the visit-only-4 task (normal orientation) followed by surgery for virus delivery, then recovery and training. Upon reaching proficiency, animals begin to undergo recording sequences. A recording sequence consists of a CTR, SAL, and CNO recording in both the normal and rotated orientations. Upon completion of the visit-only-4 task (3-5 recording sequences), animals are introduced to and tested on the visit-all-8 task for an additional 3-5 recording sequences.

Prior to surgery, rats were anesthetized with isoflurane (5%) via an isoflurane vaporizer and an induction box. The animals were placed in a stereotaxic head holder with ear bars and a nose cone (David Kopf Instruments) delivering isoflurane and oxygen (1-3% isoflurane for maintenance). The rat was placed on a water heating pad at approximately 39°C, the animal's nose and nose cone were wrapped in Petflex, and ophthalmic lubricant (Puralube Vet Ointment) was applied to prevent drying of the animal's eyes during surgery. The animal's head was shaved to clear the workspace for the incision and iodine was applied to disinfect the region.

The skull was then exposed via an incision along the midline and the skin was held aside with hemostats. Bilateral craniotomies were performed to expose the cortex on each side of the midline. Lesions were made by injecting an Adeno-Associated Virus (AAV) with a human synapsin 1 promoter-driven hM4D(Gi) receptor and a red fluorescent protein (mCherry) to create CNO-induced lesions (AAV8.hSyn.hM4Di.mCherry from Duke University). Retrosplenial cortex lesions were made by injecting four sites per hemisphere using a 5 μl Hamilton Syringe and pulled glass pipette at an infusion rate of 41.5 nL/min, or ~500 nL over 12 minutes. The glass pipette was left in place for 15 minutes after each infusion. Sterile saline (0.9%) was injected subcutaneously throughout the surgery to help maintain the animal's body temperature. The anterior-posterior (AP) and medial-lateral (ML) coordinates (in mm) were measured relative to bregma, and the dorso-ventral (Z) coordinates (in mm) relative to the surface of the cortex. The stereotaxic coordinates of the injections were: (1) 500 nL at -4.475 (AP), ± 0.5 (ML), -1.8 (Z); (2) 500 nL at -5.225 (AP), ± 0.5 (ML), -2.00 (Z); (3) 500 nL at -5.975 (AP), ± 1.0 (ML), -2.25 (Z); and (4) 500 nL at -6.725 (AP), ± 1.25 (ML), -1.8 (Z) (Figure 3).

Four skull screws were then inserted into the skull anterior to the craniotomies and bound with dental cement to a light clip, which rested on the skull to allow for light attachment and thus, positional tracking during the experiment. Upon completion of the surgery, the skin surrounding the surgery site was sutured, and a triple antibiotic (Curad Triple Antibiotic Ointment) was applied topically to the surgical site. Buprenorphine was then administered to the animal to help manage pain resulting from the surgery. An antibiotic (Keflex) was administered with food for the following week and the animal was given this time to recover.

Site	A/P (mm from Bregma)	M/L (mm from Bregma)	D/V (Z), (mm from Bregma)
1	-4.475	± 0.5	1.5 - 1.8
2	-5.225	± 0.5	1.75 - 2
3	-5.975	± 1.0	2 – 2.25
4	-6.725	± 1.25	1.6 – 1.8
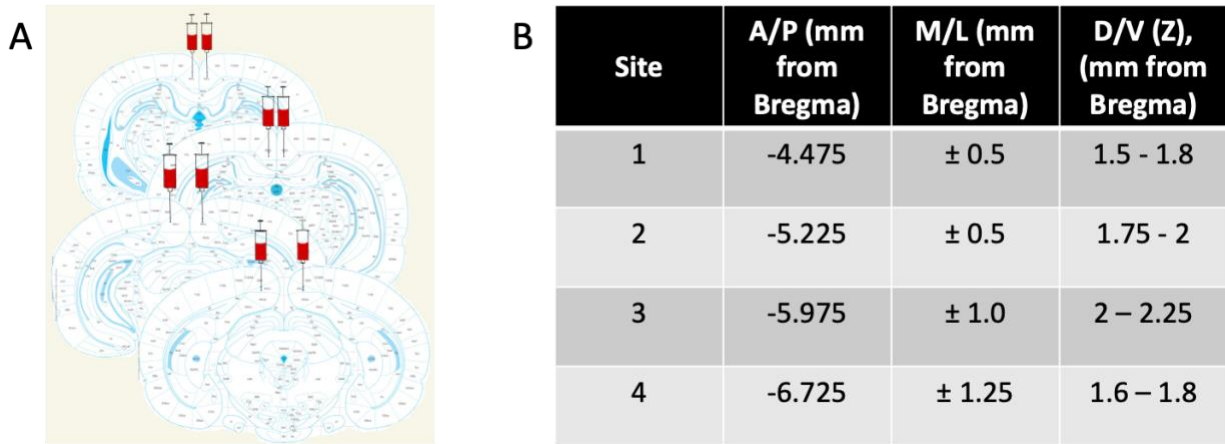
Figure 3: Target injection sites for delivery of AAV8.hSyn.hM4Di.mCherry to the RSC. (A) Schematic of injection sites adapted from the Alan Rat Brain Atlas at injection sites indicated in panel B. Injection sites in panel A from top to bottom correspond to sites 1-4 on panel B, respectively.

Behavioral Recordings and Position Tracking

After a 1-week recovery from surgery, the animals were trained for an additional 1-2 weeks to ensure adequate behavior and sufficient time for the expression of the virus (Figure 2). After this period of retraining, the animal's position was tracked using a camera that was attached to the ceiling of the recording room and pointed at the floor where the maze was positioned. LED lights were fixed to the animal's surgically implanted light clip before each

recording. Plexon's CinePlex Studio software was used to detect the LED lights, capturing the

location tracking at 60 Hz (Figure 4).

Each recording was executed under one of three experimental conditions, varying by

injection type (Figure 2). The three conditions were: (1) Control (CTR) Recording (no injection),

regular orientation + 90° rotation; (2) Saline (SAL) Recording (control recording with saline

injection), regular orientation + 90° rotation; and (3) CNO Recording (RSC inhibition via CNO

injection), regular orientation + 90° rotation (Figure 2). CNO and Saline injections were

administered intraperitoneally 45 minutes prior to the experiment at a dose of 1.4 mg/kg.

The three conditions were tested sequentially, then repeated with an alternation in the

order of the SAL and CNO experimental conditions (i.e., Week 1: 1,2,3; Week 2: 1,3,2…; Figure

2). In the rotation condition, the maze was rotated 90° in one of two directions. These rotation

conditions alternated with each recording sequence (i.e., Week 1: 1A, 2A, 3A; Week 2: 1B, 3B,

2B; Figure 2).

During the first 3-5 recording sequences (1 recording sequence = Conditions 1, 2, 3 or 1,

3, 2), the animals were recorded while performing the visit-only-4 task (Figure 1A &1B; Figure

2). Successfully collecting the reward at all four reward locations was defined as a "block."

Rewards were readministered upon completion of a block, and recording sessions continued until

the animal completed approximately 20 blocks. After these initial recording sequences, the task

was expanded and animals were introduced to all eight pathways of the TTT maze on 1-2 short

training days, during which they completed 1-2 blocks of the visit-all-8 task (Figure 1C & 1D;

Figure 2). The visit-all-8 task required the animal to collect a reward at each of the eight reward

sites on the TTT maze, with eight possible routes that lead to those sites. Upon acquisition of

rewards from all eight sites (the completion of a block), rewards were readministered at all sites

to start the subsequent block. Following this, the animals began a small period of Control

recordings with *no* rotation of the maze to become acclimated to the new task. Recording

sessions continued until the animal completed approximately 20 blocks. Finally, the recording

sequences were resumed under the visit-all-8 paradigm until the animals completed 3-5

recording sequences.
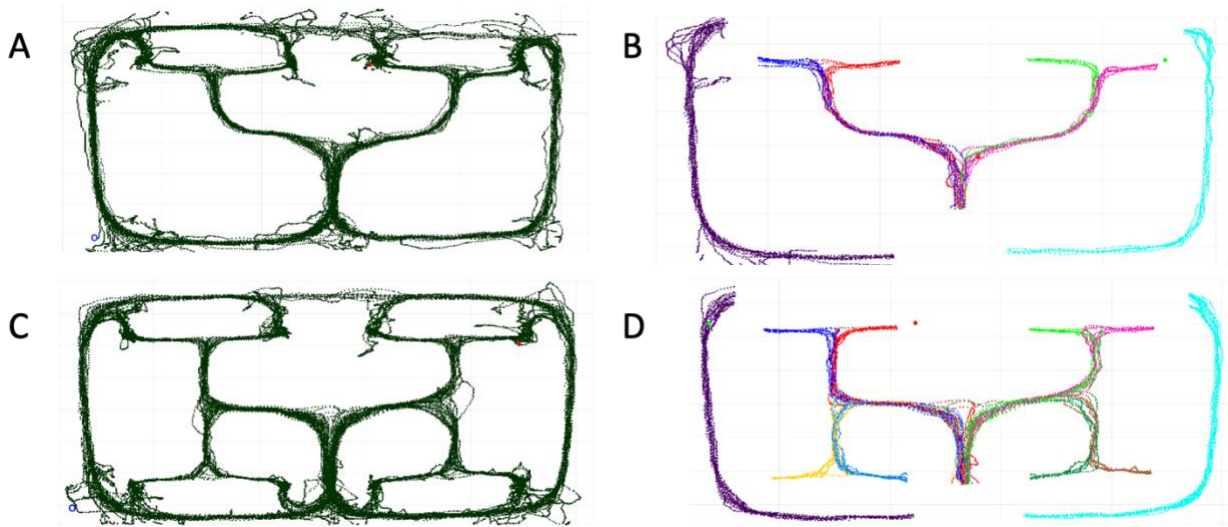
Figure 4: Tracking Data from Recordings on the TTT Maze. (A,B) Tracking data from recordings on the visit-only-4 task. (C,D) Tracking data from recordings on the visit-all-8 task. (B,D) Different colors indicate the different routes and correspond to the route numbers as labeled in Figure 1B & 1D.

Histology and Microscopy

After completion of the experiment, animals were placed under deep anesthesia (5%

Isoflurane) and administered 1.0 mL pentobarbital (FATAL-PLUS) via intraperitoneal injection

to induce lethal overdose. The rats were then perfused via a peristaltic pump through the left

ventricle with phosphate-buffered saline (PBS) and then 4% paraformaldehyde (PFA) in PBS

solution. The brains were extracted and stored in paraformaldehyde for 24hrs, then in a sucrose

solution as a cryoprotectant for at least another 24 hrs. The brains were mounted and sliced into

30 μm coronal sections via cryostat, then transferred to a multi-well tissue culture plate. The

sections were then mounted onto microscope slides, coated with Fluorogold, then cover-slipped.

Sections were imaged on a Zeiss fluorescent microscope to illuminate DAPI and the mCherry reporter from the DREADDs virus. Sections were then evaluated using the ZEN software (Zeiss).

<u>Data Analysis and Analytical Approach</u>

A custom code and user interface written in MATLAB were used for the behavioral analysis of the Triple T maze. It was used to label individual routes and blocks, as well as extract valuable behavioral data used in the analysis of this experiment.

To investigate the role of the RSC on the TTT maze tasks, we examined variance between the SAL and CNO injection conditions for a variety of behavioral variables across two different timelines. One analysis (Mann-Whitney U Test) was done between the first administration of the SAL injection and the first administration of the CNO injection ("Day 1") for both orientations of the maze. The second analysis was conducted between averages across the first three administrations of the SAL injection and the first three administrations of the CNO injection ("3 Days") for both orientations of the maze.

To gauge differences in the animals' task performance and alternation behavior we analyzed a variety of behavioral variables. The behavioral variables included: mean errors per block, where an error is defined as a route traversal that did not result in the acquisition of a reward, and a block is defined as collection of all four or eight rewards in the given task followed by the replenishment of the rewards to begin a new block; proportion of perfect blocks, which is the proportion of total blocks that had no errors; the probability of alternation at each specific turn and across analogous turns; and the probability of second order alternation at each specific turn and across analogous turns. We defined an occurrence of second order alternation as alternation behavior that occurs across four, rather than two, sequential runs. That is, alternation

at a given turn location would be, for example, a left turn followed by a right turn (L-R). Meanwhile, an instance of second order alternation at a given turn location would be, for example, two left turns followed by two right turns (L-L-R-R).

DREADDs Expression

The virus that was injected into the retrosplenial cortex (AAV8.hSyn.hM4Di.mCherry) at the eight injection sites (See Methods) contains a red fluorescent protein (mCherry), so sections were assessed for fluorescence via a fluorescent microscope (Zeiss) to determine the extent of viral expression (Figure 5). Strong bilateral expression was observed in the animals for which the histological procedures were completed (n=2; Figure 5). Other animals used in this experiment have yet to be perfused because they are currently being used for additional experiments. Quantification of viral expression has yet to be completed at the time of this writing.
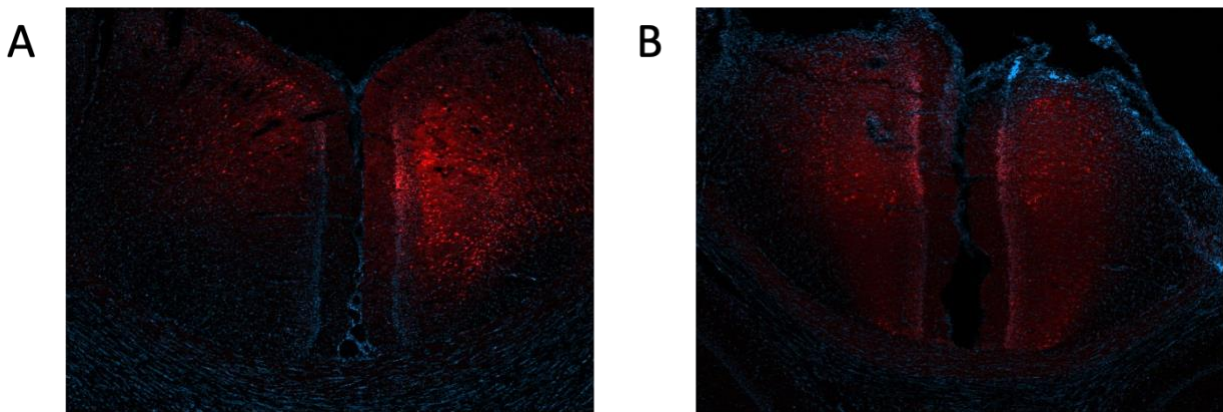
Figure 5: Expression of AAV8.hSyn.hM4Di.mCherry in the RSC. Coronal sections imaged under Zeiss fluorescent microscope. Early analysis of fluorescence indicates strong expression in the RSC. Blue fluorescence is DAPI, red fluorescence indicates viral expression (mCherry reporter). Panels A and B are images from two different animals (n=2).

Analysis

To investigate differences in the animals' task performance with inhibition of the RSC, we assessed the errors per block and proportion of perfect blocks under each of the TTT iterations. To investigate the effects of RSC inhibtion on alternation behavior, we assessed the probability of alternation at each turn specifically and across analogous turns, as well as the probability of second order alternation amongst the same turn specifications. These behavioral

variables were analyzed across six animals for the visit-only-4 task and four animals for the visit-all-8 task (Table 1; Figure 6A & 6D). One animal was excluded from analysis due to a permanent lesion lateral of the retrosplenial cortex revealed through histology.

In the visit-only-4 task, no significant differences were revealed between the CNO and SAL injection conditions in either of the two maze orientations for any of the behavioral variables analyzed (Table 1). In the visit-all-8 task on the normal orientation, however, Mann-Whitney U-test revealed a significant difference in the proportion of perfect blocks between the two injection conditions on the first injection day (p=0.0286; Figure 6A & 6B). Differences in the proportion of perfect blocks between the two injection conditions approached significance across the first three injections on the normal orientation (Mann-Whitney U Test, p=0.0571; Figure 6A & 6C). This is notable because the moderate effect of CNO injection on the first recording day became less robust over time. No significant differences were discovered among any of the other behavioral variables in the normal orientation, nor amongst any of the behavioral variables on the rotated orientation of the visit-all-8 task (Figure 6A & 6D).

Tables 1A & 1B: Results from Visit-Only-4 Task. Mean across animals (n=6) for each behavioral variable analyzed. Mann Whitney U test results comparing SAL to CNO for each variable analyzed. Means and p-values for "Day 1" data (first injection of SAL/CNO) and across first "3 Days" (averages across first three injections of SAL/CNO). (A) Results for the visit-only-4 task on the normal orientation of the maze. (B) Results for the visit-only-4 task on the rotated orientation of the maze.
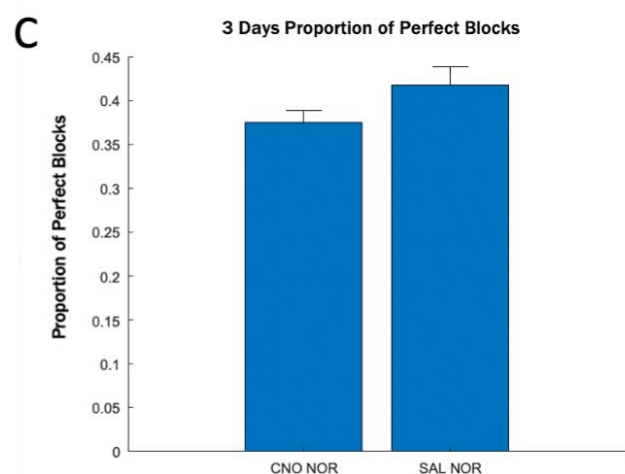
A

Variables (NORMAL CONDITION)	Mean Across Animals Day 1 – CNO NORMAL	Mean Across Animals Day 1 – SAL NORMAL	U test (p) Day 1	Mean Across Animals 3 Days – CNO NORMAL	Mean Across Animals 3 Days – SAL NORMAL	U Test (p) 3 Days
Errors/Block	0.8106 ± 0.3868	0.7376 ± 0.3023	0.7316	0.7252 ± 0.1989	0.6793 ± 0.2040	0.5887
Proportion of Perfect Blocks	0.4673 ± 0.1529	0.5787 ± 0.1472	0.1429	0.5475 ± 0.0813	0.5889 ± 0.0719	0.3939
Probability of Alternation at Turn 1	0.8634 ± 0.0400	0.8779 ± 0.0377	0.6991	0.8676 ± 0.0481	0.8442 ± 0.0359	0.4848
Probability of Alternation At Any Turn 3	0.5769 ± 0.0210	0.5497 ± 0.0335	0.1797	0.5607 ± 0.0241	0.5737 ± 0.0304	0.5886
Probability of Alternation at Specific Turn 3	0.8452 ± 0.0562	0.8548 ± 0.0412	0.6991	0.8630 ± 0.0417	0.8709 ± 0.0313	1
Probability of 2nd Order Alternation at Turn 1	0.2659 ± 0.0844	0.2263 ± 0.0645	0.4848	0.2549 ± 0.0890	0.2910 ± 0.0590	0.6991
Probability of 2nd Order Alternation at Any Turn 3	0.2583 ± 0.0861	0.2316 ± 0.0648	0.6991	0.2294 ± 0.0651	0.2154 ± 0.0501	0.7835
Probability of 2nd Order Alternation at Specific Turn 3	0.2661 ± 0.0954	0.2589 ± 0.0762	0.9372	0.2396 ± 0.0747	0.2255 ± 0.0567	0.9004

B

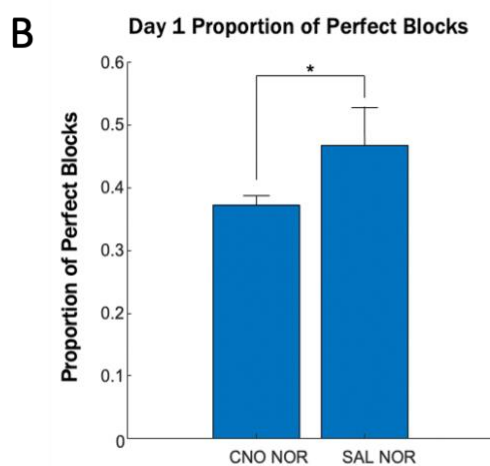| Variables (ROTATION CONDITION)	Mean Across Animals Day 1 – CNO ROTATION	Mean Across Animals Day 1 – SAL ROTATION	U test (p) Day 1	Mean Across Animals 3 Days – CNO ROTATION	Mean Across Animals 3 Days – SAL ROTATION	U Test (p) 3 Days
Errors/Block	0.8795 ± 0.3261	1.0811 ± 1.0969	0.5887	1.2677 ± 0.3618	1.0010 ± 0.4311	0.3095
Proportion of Perfect Blocks	0.5030 ± 0.1512	0.4988 ± 0.2143	1	0.4524 ± 0.0924	0.4484 ± 0.1235	0.8182
Probability of Alternation at Turn 1	0.7994 ± 0.0732	0.8349 ± 0.0699	0.6991	0.8015 ± 0.0343	0.8123 ± 0.0484	0.9372
Probability of Alternation At Any Turn 3	0.6043 ± 0.0701	0.6162 ± 0.0598	0.4848	0.6040 ± 0.0396	0.6121 ± 0.0254	0.9372
Probability of Alternation at Specific Turn 3	0.8381 ± 0.0703	0.8161 ± 0.1115	0.8182	0.7953 ± 0.0526	0.8083 ± 0.0696	0.9372
Probability of 2nd Order Alternation at Turn 1	0.3709 ± 0.1457	0.3087 ± 0.1121	0.4848	0.3566 ± 0.0766	0.3342 ± 0.0802	0.6991
Probability of 2nd Order Alternation at Any Turn 3	0.2536 ± 0.1050	0.2656 ± 0.1009	1	0.2828 ± 0.0800	0.2885 ± 0.0827	0.8182
Probability of 2nd Order Alternation at Specific Turn 3	0.2790 ± 0.1181	0.2877 ± 0.1104	0.9372	0.2948 ± 0.0458	0.3199 ± 0.0948	0.6991

A

Variables (NORMAL CONDITION)	Mean Across Animals Day 1 – CNO NORMAL	Mean Across Animals Day 1 – SAL NORMAL	U test (p) Day 1	Mean Across Animals 3 Days – CNO NORMAL	Mean Across Animals 3 Days – SAL NORMAL	U Test (p) 3 Days
Errors Per Block	1.5393 ± 0.2717	1.4940 ± 0.3572	0.9143	1.8430 ± 0.1682	1.6308 ± 0.0387	0.3429
Proportion of Perfect Blocks	0.3727 ± 0.0143	0.4678 ± 0.0608	**0.0286**	0.3755 ± 0.0131	0.4180 ± 0.0205	0.0571
Probability of Alternation at Turn 1	0.9094 ± 0.0417	0.9204 ± 0.0335	0.6857	0.9006 ± 0.0176	0.9174 ± 0.0217	0.4857
Probability of Alternation at Any Turn 2	0.5368 ± 0.0445	0.5420 ± 0.0122	0.4857	0.5467 ± 0.0154	0.5480 ± 0.0096	1
Probability of Alternation at Specific Turn 2	0.8085 ± 0.0394	0.8276 ± 0.0410	0.6857	0.7976 ± 0.0463	0.8279 ± 0.0520	0.4857
Probability of Alternation at Any Turn 3	0.5183 ± 0.0175	0.5132 ± 0.0367	1	0.4908 ± 0.0293	0.5162 ± 0.0296	0.4857
Probability of Alternation at Specific Turn 3	0.8681 ± 0.0277	0.8618 ± 0.0364	0.8857	0.8510 ± 0.0253	0.8677 ± 0.0240	0.2000
Probability of 2nd Order Alternation at Turn 1	0.1685 ± 0.0799	0.1430 ± 0.0575	0.6857	0.1786 ± 0.0355	0.1531 ± 0.0419	0.4857
Probability of 2nd Order Alternation at Any Turn 2	0.6684 ± 0.2319	0.6984 ± 0.2849	0.7429	0.3915 ± 0.0732	0.4607 ± 0.1636	0.6857
Probability of 2nd Order Alternation at Specific Turn 2	0.3511 ± 0.0550	0.3093 ± 0.0610	0.6857	0.3572 ± 0.0747	0.3071 ± 0.0832	0.4857
Probability of 2nd Order Alternation at Any Turn 3	0.2143 ± 0.0546	0.2132 ± 0.0578	1	0.2388 ± 0.0366	0.2132 ± 0.0366	0.2000
Probability of 2nd Order Alternation at Specific Turn 3	0.2232 ± 0.0401	0.2474 ± 0.0826	0.8857	0.2579 ± 0.0450	0.2331 ± 0.0476	0.3429

B

Day 1 Proportion of Perfect Blocks

C

3 Days Proportion of Perfect Blocks

D

Variables (ROTATION CONDITION)	Mean Across Animals Day 1 – CNO ROTATION	Mean Across Animals Day 1 – SAL ROTATION	U test (p) Day 1	Mean Across Animals 3 Days - CNO ROTATION	Mean Across Animals 3 Days – SAL ROTATION	U Test (p) 3 Days
Errors Per Block	5.9101 ± 5.8420	4.9211 ± 5.2438	0.3429	2.5216 ± 0.1449	2.1087 ± 0.3963	0.2000
Proportion of Perfect Blocks	0.2952 ± 0.1706	0.3053 ± 0.1765	0.6571	0.4044 ± 0.0284	0.3886 ± 0.0817	0.9429
Probability of Alternation at Turn 1	0.8507 ± 0.0404	0.8343 ± 0.1203	0.8857	0.8808 ± 0.0347	0.9167 ± 0.0094	0.2000
Probability of Alternation at Any Turn 2	0.6379 ± 0.1193	0.5519 ± 0.0214	0.1143	0.5633 ± 0.0149	0.5377 ± 0.0129	0.0571
Probability of Alternation at Specific Turn 2	0.5919 ± 0.3435	0.6535 ± 0.2561	0.6857	0.7761 ± 0.0276	0.8055 ± 0.0225	0.3429
Probability of Alternation at Any Turn 3	0.5640 ± 0.0635	0.5585 ± 0.0214	0.3429	0.5251 ± 0.0292	0.5248 ± 0.0120	0.5714
Probability of Alternation at Specific Turn 3	0.7628 ± 0.1704	0.7966 ± 0.1271	1	0.8525 ± 0.0275	0.8760 ± 0.0238	0.2000
Probability of 2nd Order Alternation at Turn 1	0.2870 ± 0.0695	0.2600 ± 0.1452	0.4857	0.2253 ± 0.0629	0.1561 ± 0.0150	0.1143
Probability of 2nd Order Alternation at Any Turn 2	0.2473 ± 0.1551	0.2714 ± 0.0761	1	0.3708 ± 0.0254	0.3645 ± 0.0485	0.8857
Probability of 2nd Order Alternation at Specific Turn 2	0.2825 ± 0.1745	0.3524 ± 0.0326	1	0.3616 ± 0.0282	0.3344 ± 0.0193	0.3429
Probability of 2nd Order Alternation at Any Turn 3	0.2016 ± 0.0649	0.2715 ± 0.1202	0.4857	0.2269 ± 0.0473	0.1893 ± 0.0350	0.4857
Probability of 2nd Order Alternation at Specific Turn 3	0.2529 ± 0.0602	0.2635 ± 0.0668	0.8857	0.2430 ± 0.0409	0.2123 ± 0.0503	0.3429

Figure 6: Results from Visit-All-8 Task. (A-C) Results from the normal orientation of the maze. (A,D) Mean across animals (n=4) for each behavioral variable analyzed. Mann Whitney U test results comparing SAL to CNO for each variable analyzed. Means and p-values for "Day 1" data (first injection of SAL/CNO) and across first "3 Days" (averages across first three injections of SAL/CNO). (B) Proportion of perfect blocks Day 1 (Mann Whitney U Test, p=0.0286). (C) Proportion of perfect blocks across 3 Days (Mann Whitney U Test, p=0.0571). (D) Results for the visit-all-8 task on the rotated orientation of the maze.

DISCUSSION

Previous studies have utilized T-maze alternation tasks and the eight-arm radial maze as tests of working memory because animals are required to remember their previous decision to efficiently perform the task. The TTT maze and its associated tasks take these simple tasks and expand them, creating a uniquely complex working memory task that requires the animal to remember up to seven of its previous decisions to solve the tasks with maximum efficiency. Notably, the TTT maze and its tasks integrate the animals' alternation behavior but cannot be solved with alternation alone. To most effectively perform the TTT tasks, animals must utilize their spatial working memory as they make informed decisions based on their previous route traversals.

Temporary inactivation of the RSC has been shown to significantly impair standard alternation on the T-maze upon maze rotation (Nelson et al., 2015a). For this reason, we analyzed the variance in alternation behavior between injection conditions through a variety of variables. Interestingly, on the TTT tasks, alternation behavior was largely maintained in both the SAL and CNO injection conditions in every iteration of the TTT maze (Table 1; Figure 6A & 6D). Furthermore, we observed no significant difference in alternation behavior between the two injection conditions on either orientation, suggesting little effect of the RSC inhibition on alternation behavior in the TTT maze paradigm (Table 1; Figure 6A & 6D).

Throughout the recordings, we observed that the animals had a tendency to alternate in the second degree (L-L-R-R or R-R-L-L) to solve the maze, so we investigated differences in this behavior for the SAL and CNO injection conditions. There was no significant difference between the two groups in alternation behavior in any of the task iterations, but the occurrence of

second order alternation itself is a finding worth noting (Table 1; Figure 6A & 6D). Second order alternation is a serendipitous finding and the further interpretation of it requires more experimentation, but we note that the development of this behavior perhaps simplifies the navigational problem by breaking the eight locations into four quadrants. That is, a spatial organization that facilitates task completion is observed. However, statistical verification of the occurrence of second order alternation has yet to be completed at the time of this writing.

We found a significant difference between the Day 1 proportion of perfect blocks on the normal orientation of the visit-all-8 task (p=0.0286; Figure 6A & 6B). This effect became less robust across three days on the normal orientation (p=0.0571; Figure 6A & 6C). These results can be described as a moderate effect on task performance, suggesting that the RSC is a contributor, but not essential, to the performance of this task in any of its iterations. Nevertheless, transient lesion of RSC results in a significant deficit in task performance on Day 1 of the visit-all-8 task (Figure 6A & 6B). Notably, we see a significant impairment exclusively when the animals have only just learned to modify and expand their strategies to solve the new, more challenging task, suggesting that inhibition of the RSC may have a more robust effect on recently learned navigational tasks.

The present technique, chemogenetic manipulation, creates a more subtle manipulation of the RSC. Chemogenetic manipulations are known to be less extensive than other lesions (Smith et al., 2016). Thus, it is possible that a more extensive inactivation of the RSC could yield stronger results. It is also important to note that full scale quantification of viral expression has yet to be completed at the time of this writing. Quantification and evaluation of expression for all animals may reveal possible reasons for variation in behavior across animals, as well as confirm that CNO induced lesions did, in fact, inhibit neurons in the retrosplenial cortex for all animals.

The visit-all-8 task is the more complex version of the TTT tasks and allows mild impairments to be detected using our inactivation technique. Furthermore, outside of the role of the RSC, the task revealed novel features of behavior that can be examined in future studies. These novel features include the development, or lack thereof, of alternation at an intersection where the animal previously did not have a choice. They also include the potential emergence, or lack thereof, of second order alternation behavior. Neither of these variables is impacted by transient lesion of the RSC, but it is possible that a more complete inactivation of the RSC or inactivation of other regions within this circuit may reveal an effect on second order alternation. Additionally, the data from only four animals was analyzed for the visit-all-8 task and six animals for the visit-only-4 task, so more statistical power by means of more subjects may also reveal more robust impairments in the task performance or differences in alternation behavior.

Ultimately, in this study we attempted to maximize the complexity of the navigational task to detect the contribution of the RSC to a well learned spatial working memory task. This design was successful as a moderate impairment in task performance was observed under the most difficult circumstance of the experiment–the recently learned, most challenging version of the task–suggesting that the retrosplenial cortex contributes to performance on a challenging spatial working memory task and may be particularly important in performance on recently learned navigational tasks.

This thesis is co-authored with Johnson, Alexander; Xu, Jingyue (Charles); and Nitz, Douglas. The thesis author is the primary investigator and author of this material.

REFERENCES

Ainge, J. A., Tamosiunaite, M., Woergoetter, F., & Dudchenko, P. A. (2007). Hippocampal CA1
    Place Cells Encode Intended Destination on a Maze with Multiple Choice Points. *Journal of
    Neuroscience*, *27*(36), 9769–9779. https://doi.org/10.1523/JNEUROSCI.2011-07.2007

Alexander, A. S., & Nitz, D. A. (2015b). Retrosplenial cortex maps the conjunction of internal
    and external spaces. *Nature Neuroscience*, *18*(8), 1143–1151.
    https://doi.org/10.1038/nn.4058

Alexander, A. S., & Nitz, D. A. (2017). Spatially Periodic Activation Patterns of Retrosplenial
    Cortex Encode Route Sub-spaces and Distance Traveled. *Current Biology*, *27*(11), 1551-
    1560.e4. https://doi.org/10.1016/j.cub.2017.04.036

Armbruster, B. N., Li, X., Pausch, M. H., Herlitze, S., & Roth, B. L. (2007). Evolving the lock to
    fit the key to create a family of G protein-coupled receptors potently activated by an inert
    ligand. *Proceedings of the National Academy of Sciences*, *104*(12), 5163-5168.
    https://doi.org/10.1073/pnas.0700293104

Blair, T., & Sharp, E. (1995) Anticipatory Head Direction Signals in Anterior Thalamus:
    Evidence for a Thalamocortical Circuit That Integrates Angular Head Motion to Compute
    Head Direction. *The Journal of Neuroscience*, 15(9), 6260-6270.
    https://doi.org/10.1523/JNEUROSCI.15-09-06260.1995

Brennan, E. K., Jedrasiak-Cape, I., Kailasa, S., Rice, S. P., Sudhakar, S. K., & Ahmed, O. J.
    (2021). Thalamus and claustrum control parallel layer 1 circuits in retrosplenial cortex.
    ELife, *10*, e62207. https://doi.org/10.7554/eLife.62207

Chen, L.L., Lin, LH., Green, E.J., Barnes, C.A., & McNaughton, B.L. (1994) Head-direction
    cells in the rat posterior cortex. *Exp Brain Res*. 16. https://doi.org/10.1007/BF00243212

Cho, J., & Sharp, P. E. (2001). Head direction, place, and movement correlates for cells in the rat
    retrosplenial cortex. *Behavioral Neuroscience, 115*(1), 3–25. https://doi.org/10.1037/0735-
    7044.115.1.3

Clark, B. J., Bassett, J. P., Wang, S. S., & Taube, J. S. (2010). Impaired Head Direction Cell
    Representation in the Anterodorsal Thalamus after Lesions of the Retrosplenial Cortex.
    Journal of Neuroscience, *30*(15), 5289–5302. https://doi.org/10.1523/JNEUROSCI.3380-
    09.2010

Fournier, D. I., Monasch, R. R., Bucci, D. J., & Todd, T. P. (2020). Retrosplenial cortex damage impairs unimodal sensory preconditioning. *Behavioral Neuroscience*, *134*(3), 198–207. https://doi.org/10.1037/bne0000365

Franco, L. M., & Goard, M. J. (2021). A distributed circuit for associating environmental context with motor choice in retrosplenial cortex. *Science Advances*, *7*(35), eabf9815. https://doi.org/10.1126/sciadv.abf9815

Frank, L. M., Brown, E. N., & Wilson, M. (2000). Trajectory Encoding in the Hippocampus and Entorhinal Cortex. *Neuron*, *27*(1), 169–178. https://doi.org/10.1016/S0896-6273(00)00018-0

Grieves, R. M., Wood, E. R., & Dudchenko, P. A. (2016). Place cells on a maze encode routes rather than destinations. *ELife*, *5*, e15986. https://doi.org/10.7554/eLife.15986

Keene, C. S., & Bucci, D. J. (2008a). Contributions of the retrosplenial and posterior parietal cortices to cue-specific and contextual fear conditioning. *Behavioral Neuroscience, 122*(1), 89–97. https://doi.org/10.1037/0735-7044.122.1.89

Keene, C. S., & Bucci, D. J. (2008b). Neurotoxic lesions of retrosplenial cortex disrupt signaled and unsignaled contextual fear conditioning. *Behavioral neuroscience*, *122*(5), 1070–1077. https://doi.org/10.1037/a0012895

Kügler, S., Kilic, E. & Bähr, M. (2003). Human synapsin 1 gene promoter confers highly neuron-specific long-term transgene expression from an adenoviral vector in the adult rat brain depending on the transduced area. *Gene Therapy,* 10, 337–347. https://doi.org/10.1038/sj.gt.3301905

Lahr, M., & Donato, F. (2020). Navigation: How Spatial Cognition Is Transformed into Action. *Current Biology*, *30*(10), R430–R432. https://doi.org/10.1016/j.cub.2020.03.069

Mizumori, S. J., & Williams, J. D. (1993). Directionally selective mnemonic properties of neurons in the lateral dorsal nucleus of the thalamus of rats. *The Journal of neuroscience : the official journal of the Society for Neuroscience*, *13*(9), 4015–4028. https://doi.org/10.1523/JNEUROSCI.13-09-04015.1993

Nelson, A. J. D., Hindley, E. L., Pearce, J. M., Vann, S. D., & Aggleton, J. P. (2015). The effect of retrosplenial cortex lesions in rats on incidental and active spatial learning. *Frontiers in Behavioral Neuroscience*, *9*. https://doi.org/10.3389/fnbeh.2015.00011

Nelson, A. J. D., Powell, A. L., Holmes, J. D., Vann, S. D., & Aggleton, J. P. (2015). What does spatial alternation tell us about retrosplenial cortex function? *Frontiers in Behavioral Neuroscience*, *9*. https://doi.org/10.3389/fnbeh.2015.00126

O'Keefe, J., & Dostrovsky, J. (1971). The hippocampus as a spatial map. Preliminary evidence from unit activity in the freely-moving rat. *Brain research*, *34*(1), 171–175. https://doi.org/10.1016/0006-8993(71)90358-1

Olson, J. M., Li, J. K., Montgomery, S. E., & Nitz, D. A. (2020). Secondary Motor Cortex Transforms Spatial Information into Planned Action during Navigation. *Current biology: CB*, *30*(10), 1845–1854.e4. https://doi.org/10.1016/j.cub.2020.03.016

Olton, D. S., & Samuelson, R. J. (1976). Remembrance of places passed: spatial memory in rats. *Journal of experimental psychology: Animal behavior processes*, *2*(2), 97. https://doi.org/10.1037/0097-7403.2.2.97

Olton, D. S. (1986). Hippocampal function and memory for temporal context. *The Hippocampus* (pp. 281-298). Springer, Boston, MA.

Pothuizen, H. H. J., Aggleton, J. P., & Vann, S. D. (2008). Do rats with retrosplenial cortex lesions lack direction? *European Journal of Neuroscience*, *28*(12), 2486-2498. https://doi.org/10.1111/j.1460-9568.2008.06550.x

Quirk, J., Muller, U., Kubie, J. L., & Ranck, B. (1992). The Positional Firing Properties of Medial Entorhinal Neurons: Description and Comparison with Hippocampal Place Cells. *Journal of Neuroscience,* 12(5), 1945-1963. https://doi.org/10.1523/jneurosci.12-05-01945.1992.

Sharp, P. E., & Green, C. (1994). Spatial correlates of firing patterns of single cells in the subiculum of the freely moving rat. *Journal of Neuroscience*, *14*(4), 2339-2356. https://doi.org/10.1523/JNEUROSCI.14-04-02339.1994

Shibata, H., Kondo, S., & Naito, J. (2004). Organization of retrosplenial cortical projections to the anterior cingulate, motor, and prefrontal cortices in the rat. *Neuroscience research*, *49*(1), 1-11. https://doi.org/10.1016/j.neures.2004.01.005

Smith, D. M., Barredo, J., & Mizumori, S. J. Y. (2012). Complimentary roles of the hippocampus and retrosplenial cortex in behavioral context discrimination. *Hippocampus*, *22*(5), 1121–1133. https://doi.org/10.1002/hipo.20958

Smith, K. S., Bucci, D. J., Luikart, B. W., & Mahler, S. V. (2016). DREADDS: Use and application in behavioral neuroscience. *Behavioral Neuroscience, 130*(2), 137–155. https://doi.org/10.1037/bne0000135

Sugar, J., Witter, M. P., van Strien, N. M., & Cappaert, N. L. (2011). The retrosplenial cortex: intrinsic connectivity and connections with the (para) hippocampal region in the rat. An interactive connectome. *Frontiers in neuroinformatics*, *5*, 7. https://doi.org/10.3389/fninf.2011.00007

Sul, J. H., Jo, S., Lee, D., & Jung, M. W. (2011). Role of rodent secondary motor cortex in value-based action selection. *Nature neuroscience*, *14*(9), 1202-1208. https://doi.org/10.1038/nn.2881

Taube, S. (1995a). Head Direction Cells Recorded in the Anterior Thalamic Nuclei of Freely Moving Rats. *Journal of Neuroscience,* 15 (1), https://doi.org/10.1523/JNEUROSCI.15-01-00070.1995

Taube, J.S. (1995b), Place cells recorded in the parasubiculum of freely moving rats. *Hippocampus*, 5: 569-583. https://doi.org/10.1002/hipo.450050608

van Groen, T., Kadish, I., & Wyss, J. M. (2004). Retrosplenial cortex lesions of area Rgb (but not of area Rga) impair spatial learning and memory in the rat. *Behavioural Brain Research*, *154*(2), 483–491. https://doi.org/10.1016/j.bbr.2004.03.016

Vann, S. D., & Aggleton, J. P. (2004). Testing the importance of the retrosplenial guidance system: Effects of different sized retrosplenial cortex lesions on heading direction and spatial working memory. *Behavioural Brain Research*, *155*(1), 97–108. https://doi.org/10.1016/j.bbr.2004.04.005

Vann, S. D., Aggleton, J. P., & Maguire, E. A. (2009). What does the retrosplenial cortex do? *Nature Reviews Neuroscience*, *10*(11), 792–802. https://doi.org/10.1038/nrn2733

Vogt, B. A., & Peters, A. (1981). Form and distribution of neurons in rat cingulate cortex: areas 32, 24, and 29. *The Journal of Comparative Neurology*, *195*(4), 603–625. https://doi.org/10.1002/cne.901950406

Vogt, B. A., & Miller, M. W. (1983). Cortical connections between rat cingulate cortex and visual, motor, and postsubicular cortices. *Journal of Comparative Neurology*, *216*(2), 192-210. https://doi.org/10.1002/cne.902160207

Vogt, B. A., Vogt, L., & Farber, N. B. (2004). Cingulate cortex and disease models. *The rat nervous system*, *3*, 705-727.

Wood, E. R., Dudchenko, P. A., Robitsek, R. J., & Eichenbaum, H. (2000). Hippocampal Neurons Encode Information about Different Types of Memory Episodes Occurring in the Same Location. *Neuron*, *27*(3), 623–633. https://doi.org/10.1016/S0896-6273(00)00071-4

Wyss, J. M., & Van Groen, T. (1992). Connections between the retrosplenial cortex and the hippocampal formation in the rat: a review. *Hippocampus*, *2*(1), 1-11. https://doi.org/10.1002/hipo.450020102

Yamawaki, N., Li, X., Lambot, L., Ren, L. Y., Radulovic, J., & Shepherd, G. M. G. (2019). Long-range inhibitory intersection of a retrosplenial thalamocortical circuit by apical tuft-targeting CA1 neurons. *Nature Neuroscience*, *22*(4), 618–626. https://doi.org/10.1038/s41593-019-0355-x

Yamawaki, N., Radulovic, J., & Shepherd, G. M. G. (2016). A Corticocortical Circuit Directly Links Retrosplenial Cortex to M2 in the Mouse. *The Journal of Neuroscience*, *36*(36), 9365–9374. https://doi.org/10.1523/JNEUROSCI.1099-16.2016